Journal of
Materials Chemistry C

ROYAL SOCIETY
OF CHEMISTRY

PAPER

View Article Online
View Journal

Check for updates

Cite this: DOI: 10.1039/d0tc00308e

Photo-crosslinkable second order nonlinear AB_2-type monomers: convenient synthesis and enhanced NLO thermostability†

Ruifang Wang,[a] Ziyao Cheng,[a] Xiaocong Deng,[a] Wenjing Zhao,[a] Qianqian Li[a] and Zhen Li*[ab]

Received 16th January 2020,
Accepted 17th March 2020

DOI: 10.1039/d0tc00308e

rsc.li/materials-c

In this article, two AB_2-type second-order nonlinear optical monomers (**DN-SH** and **DS-SH**) containing two double bonds and one thiol group, respectively, were synthesized successfully. These two monomers could be *in situ* photo-crosslinked *via* a thiol–ene click reaction under 365 nm UV light without a photoinitiator after poling. Thanks to the photo-crosslinking process of thin films, the thermostability of the second-order nonlinear optical property was much enhanced. **DS-SH** exhibited a larger NLO effect and better NLO thermostability than **DN-SH**, because of the introduction of sulfonyl-based chromophores which can decrease the electrostatic interaction between nitro-based chromophore moieties. $T_{80\%}$ of the photo-crosslinked **DS-SH** films increased to 112.5 °C, much higher than that of uncrosslinked ones (75 °C), while $T_{80\%}$ of **DN-SH** films increased from 58 to 95 °C. More excitedly, the doped thin films of **DN-SH** and **DS-SH** at different molar ratios (1 : 1, 2 : 1, and 1 : 2) showed better NLO properties (123, 122, and 114 pm V^{-1}, respectively) after photo-crosslinking than single **DN-SH** (89 pm V^{-1}) and **DS-SH** (108 pm V^{-1}) respectively.

Introduction

Second-order nonlinear optical (NLO) materials have been widely studied in the past few decades, because of their extensive applications such as in high-speed electrooptic modulation, frequency doubling, data storage, telecommunications and so on.[1] Compared to inorganic nonlinear materials having a low electrooptical coefficient, high dielectric constant and difficulties in crystal growth, organic nonlinear materials have attracted great attention because of their definite advantages of ultra-fast response speed, large NLO properties and convenient processability.[2] In order to meet the requirement for practical applications, NLO materials should not only have large NLO properties, but also good thermal and optical stability.[3] Therefore, many efforts have been made to improve the stability of NLO materials. One of the methods is to synthesize polymers with high glass transition temperatures, such as polyimides, especially when chromophore moieties were attached to the polymer backbone.[4] However, there are strict requirements for the thermostability of molecules and chromophores, which would be degraded at such a high temperature of poling. Another method to improve the NLO stability is to create Diels–Alder thermal-crosslinkable networks, such as trismaleimides and dienes, which can react partly at a baking temperature of 50 °C according to their highly reactive nature.[5] However, it is hard to control the best poling temperature, which strongly relies on the balance between glass transition temperature, dissociation and crosslinking. The last method is the design of photocrosslinkable polymers (Chart S1, ESI†).[6] It has a great advantage because the photo-crosslinking process can be conducted easily during or after poling under UV light with/without photoinitiators. As early as 1994, two photo-crosslinked acrylic monomers bearing nitroazobenzene chromophores showed no relaxation for a week at 80 °C after relatively quick UV-initiated polymerization.[7] Another photo-crosslinked NLO epoxy polymer containing cinnamate-functionalized substituents was prepared successfully with improved NLO thermostability after UV curing.[8] Recently, a direct writing approach was conducted to obtain Mach–Zehnder waveguides after photo-crosslinking.[9]

Another implementation of an NLO material device is to promote the second harmonic generation (SHG) effect, characterized by d_{33}. In 2006, the concept of a ‘‘suitable isolation group’’ (SIG) was proposed by our group,[10] and then a series of systematic research studies were conducted accompanied by

---

[a] *Sauvage Centre for Molecular Science, Department of Chemistry, Wuhan University, Wuhan 430072, China. E-mail: lizhen@wh.edu.cn, lichemlab@163.com*

[b] *Institute of Molecular Aggregation Science, Tianjin University, Tianjin 300072, China*

† Electronic supplementary information (ESI) available. See DOI: 10.1039/d0tc00308e

rational molecular designs and optimized spatial configuration. In particular, the successful preparation of dendrimers, hyperbranched polymers and dendronized hyperbranched polymers efficiently translates large microscopic μβ to high macroscopic NLO properties.[11] Thus, high performance of NLO properties was achieved, up to 299 pm V^{-1} (Chart S2, ESI†), which was the best value based on azo chromophores so far. As mentioned above, we aimed to further enhance the thermostability of NLO property through a simple and controllable method, and achieve a relatively good NLO effect at the same time. Generally, the thiol–ene click reaction can be carried out efficiently with/without photoinitiators under UV light, which attracted much attention in various applications.[12] Hence, our group made a preliminary exploration by synthesizing a kind of photo-crosslinkable second-order NLO linear polymer containing double bonds which can react with pentaerythritol tetra(3-mercaptopropionate) (PETMP) under UV light (Chart S1, ESI†). As expected, the crosslinked films exhibited better thermostability of NLO property than uncrosslinked ones, demonstrating the feasibility and operability of the photo-crosslinking method by utilizing the thiol–ene click reaction in second-order nonlinear materials.[13] Thus, the photo-induced thiol–ene click reaction may be a promising method to improve the thermostability of NLO property. However, the use of a cross-linking agent (PETMP) without an NLO effect will reduce the loading density of chromophore moieties, leading to a reduction of the NLO properties. Therefore, we wonder if simply synthesized low-generation azo dendrimers can be utilized to form functionalized compounds which can be photo-crosslinked by themselves in the absence of a cross-linking agent.

In this work, we further developed this photo-crosslinking method. As shown in Fig. 1, two AB_2-type monomers, **DN-SH** and **DS-SH**, were synthesized successfully by the azide-alkyne click reaction, esterification of hydroxyl groups and reduction of disulfide bonds, in which, two double bonds and one thiol group were present on the head and tail of the chromophores respectively. Firstly, the chromophore moieties with donor–π–acceptor (D–π–A) structures can achieve noncentrosymmetric alignment through poling under a high electric field. However, molecules were easily able to return to their centrosymmetric alignment because of the strong dipole–dipole interaction between chromophore moieties without the application of an electric field.[14] Thus, 365 nm UV light was applied to initiate a photo-crosslinking process of chromophores under an electric

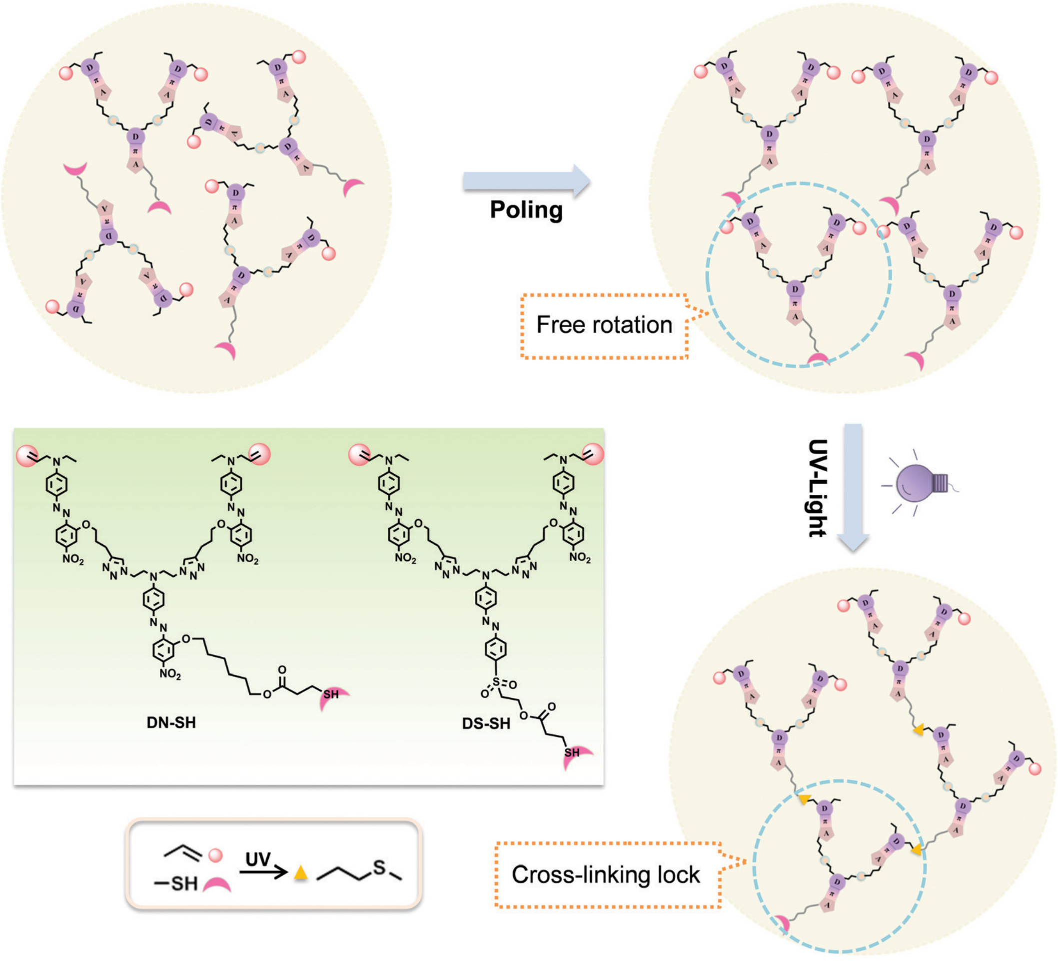

Fig. 1 Schematic illustration of the photo-crosslinking process and the structures of **DN-SH** and **DS-SH**.

field, so that free-rotating molecules can be locked by cross-linking. As a result, the thermostability of NLO property was greatly improved after photo-crosslinking in comparison with that of uncrosslinked films. The $T_{80\%}$ of **DN-SH** increased from 58 to 95 °C, and 75 to 112.5 °C for **DS-SH**. Herein, we will present the synthesis, characterization, photo-crosslinking process, and NLO properties of these new monomers in detail.

Results and discussion

Synthesis and characterization

Two photo-crosslinkable second-order nonlinear optical AB_2-type monomers **DN-SH** and **DS-SH** were prepared successfully. The carbon–carbon double bonds and thiol groups of the chromophore moieties can be crosslinked *via* the thiol–ene click reaction under UV light after poling. The specific synthetic routes and preparation procedures are shown in Scheme 1 and in the Experimental section. Taking **DN-SH** for example, firstly, we obtained an important intermediate of **DN-OH** through the Cu(I)-catalyzed azide–alkyne cycloaddition click reaction accompanied by the formation of triazole rings,[15] which can act as isolation groups to decrease strong dipole–dipole interactions between chromophores. The target monomer **DN-SH** was obtained in a satisfactory yield by another two steps, subsequent esterification of hydroxyl groups in **DN-OH** and reduction of disulfide bonds in **DS-S-S-DS**, respectively. The synthetic route of another monomer **DS-SH** is similar to that of **DN-SH** (ESI†). And these two monomers have good solubility in common polar organic solvents, such as DCM, $CHCl_3$, THF, and DMF.

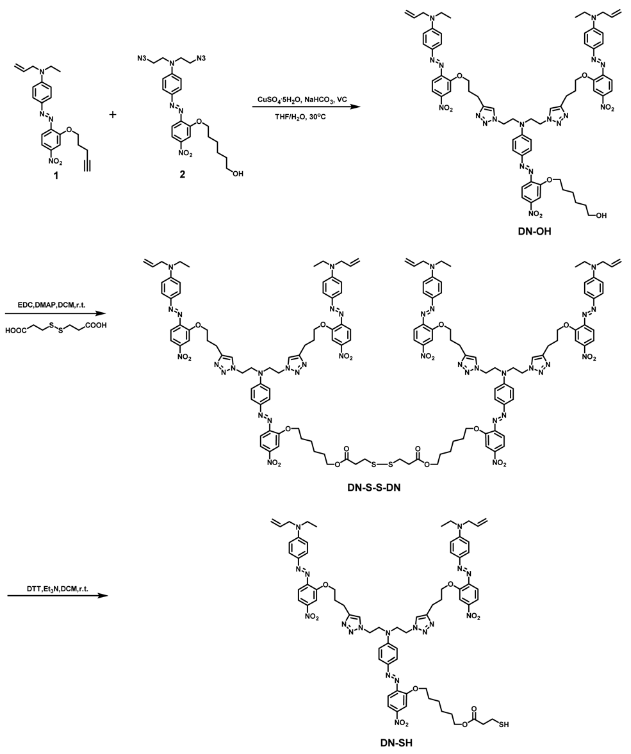

Scheme 1 Synthesis of **DN-SH**.

All target monomers and the related intermediates were well characterized by nuclear magnetic resonance (NMR) (specific analysis is shown in the Experimental section and the ESI†). Besides, high resolution mass spectrometry (HRMS) and elementary analysis (EA) were further utilized to characterize AB_2-type monomers. The calculated mass of **DN-SH** and **DS-SH** is in good accordance with the results of HRMS (Table S1, ESI†). The thermal stability of monomers was measured by thermogravimetric analysis (TGA). As shown in Table S1 (ESI†), the degradation temperatures (T_d) of **DN-SH** and **DS-SH** were about 245.9 and 216.3 °C, respectively. Generally, the temperature of nonlinear materials is below 200 °C for practical applications. The glass transition temperatures (T_g) of monomers were also investigated by differential scanning calorimetry (DSC), with the results summarized in Table S1 (ESI†). The T_g value of monomer **DS-SH** (70.5 °C) was higher than that of **DN-SH** (60.5 °C), possibly due to the introduction of sulfonyl-chromophore moieties.

The UV-vis absorption spectra of target monomers in different solvents are demonstrated in Fig. 2, with the maximum absorption wavelengths (λ_{max}) for the π–π* transitions derived from azo moieties summarized in Table 1. The λ_{max} of **DS-SH** blue-shifted in the same solvent in comparison with that of **DN-SH.** As we all know, the $\mu\beta$ value of the sulfonyl-based chromophore is lower than that of the nitro-based chromophore, thus it is normal that **DS-SH** showed better optical transparency than **DN-SH.** And the two monomers exhibited solvatochromism phenomena, that is to say, the UV-vis spectra and λ_{max} of molecules are different in different solvents, and Δ was defined as the difference between the λ_{max} values in different polar solvents of 1,4-dioxane and DMSO.[16] As shown in Table 1, **DN-SH** exhibited a larger Δ value (29 nm) than that of **DS-SH** (22 nm), indicating that the introduction of sulfonyl-based chromophores can decrease the strong dipole–dipole interactions between azo-based chromophores.

Fourier transform infrared (FT-IR) spectroscopy was performed to identify the functional groups of **DN-SH** and **DS-SH.** As shown

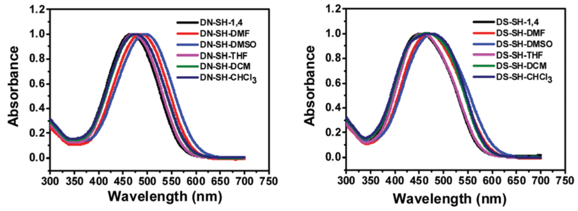

Fig. 2 UV-vis spectra of **DN-SH** and **DS-SH** in different solvents (1,4-dioxane, *N*,*N*-dimethylformamide, dimethyl sulfoxide, tetramethylene oxide, chloroform, and dichloromethane; 0.02 mg mL^{-1}).

Table 1 Maximum absorption wavelength (λ_{max}, nm) of monomers in different solvents (0.02 mg mL^{-1})

	1,4-Dioxane	$CHCl_3$	DCM	THF	DMF	DMSO	Δ
DN-SH	466	475	475	471	487	495	29
DS-SH	455	470	472	458	470	477	22

$\Delta = \lambda_{max}$ (DMSO) − λ_{max} (1,4-dioxane).

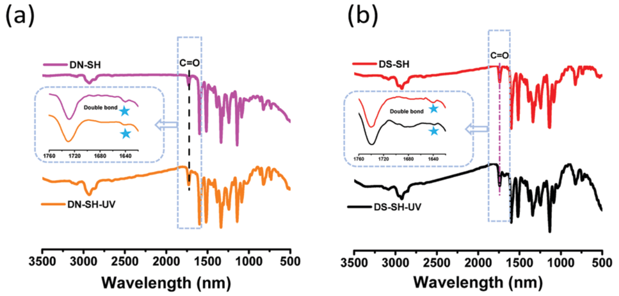

Fig. 3 FT-IR spectra of the monomers and the corresponding photo-crosslinking systems. (a) Monomer **DN-SH** was illuminated for 0 min (purple curves), and **DN-SH-UV** was illuminated for 30 min (orange curves); (b) monomer **DS-SH** was illuminated for 0 min (red curves), and **DS-SH-UV** was illuminated for 30 min (black curves).

in Fig. 3, **DN-SH** (purple curves) and **DS-SH** (red curves) both showed absorption bands associated with the carbonyl groups (at about 1739 cm^{-1}) and the nitro groups (at about 1515 and 1338 cm^{-1}). Meanwhile, a weak absorption band associated with carbon–carbon double bonds appeared at about 1640 cm^{-1}, further confirming the successful preparation of target monomers. Unfortunately, another characteristic peak of thiol groups was not observed in FT-IR spectra. There may be two main reasons for this: the content of thiol groups in the whole molecule is too low to be detected[17] and besides, the small thiol groups are wrapped in the interior of much larger monomers so that weak absorption cannot be observed.

Photo-crosslinking of AB_2-monomer films

AB_2-type monomers **DN-SH** and **DS-SH** can react with themselves through the thiol–ene click reaction under UV light. And this process can be monitored by FT-IR spectroscopy (Fig. 3). The specific operations are as follows: monomers **DN-SH** and **DS-SH** were dissolved in dichloromethane, respectively, and then the solution was coated on a KBr pellet. The FT-IR spectra of monomers with different illumination times (0 min and 30 min) were obtained. As shown in Fig. 3a, the characteristic peak of **DN-SH** at about 1640 cm^{-1}, which is ascribed to the carbon–carbon double bond, became weaker after UV exposure for 30 min, compared to initial monomers without the UV light. Similarly, the intensity of carbon–carbon double bonds stemming from **DS-SH** decreased after illuminating for 30 min (Fig. 3b). All these results demonstrated that the thiol–ene addition reaction of two monomers was conducted successfully and efficiently.

NLO properties of photo-crosslinked films

DN-SH and **DS-SH** exhibited good film-forming properties. Their solutions can be easily spin-coated into thin solid films, no matter **DN-SH** and **DS-SH** have relatively low molecular weight (1369 and 1316 respectively). Thus, their NLO properties can be tested based on the thin films conveniently. The most convenient method to study the second-order NLO property of materials is to explore the second harmonic generation SHG coefficient (d_{33}). The method to calculate d_{33} of films has been reported before.[11] The real-time poling and depoling processes were monitored accompanied by the increase of temperature at the rate of 4 °C min^{-1}. $T_{80\%}$ represents the temperature at which the SHG signal decreased by 80% of the initial value during the depoling process. Thus, the $T_{80\%}$ can be used as a parameter to judge whether NLO properties are stable or not. Generally, the higher the $T_{80\%}$ is, the better stability SHG has, which is beneficial for practical applications.

The specific photo-crosslinkable process and preparation of films are described in the Experimental section. At first, films **DN-SH1** and **DS-SH1** were measured to obtain the poling and depoling curves without UV light. As shown in Fig. S4 and S6 (ESI†), **DS-SH1** exhibited higher T_e (90 °C) compared to that of **DN-SH1** (64 °C), because of the existence of the sulfonyl-based chromophore. At the same time, the $T_{80\%}$ of **DN-SH1** and **DS-SH1** was 58 and 75 °C respectively. Next, we chose other films to conduct the photo-crosslinking process. And the photo-crosslinking process was carried out under different conditions in order to get better results. Plan A: the films (**DN-SH5** and **DS-SH3**) were heated approximately at the best poling temperature (64 and 90 °C respectively) under the electric field. After maintaining for 10 min at T_e, the poled films were irradiated for 30 min under 365 nm UV light with the voltage still being applied. Plan B: the films (**DN-SH2** and **DS-SH2**) were also heated to the best poling temperature (64 and 90 °C respectively). After maintaining for 10 min at T_e, the poled films were cooled to the room temperature with the frozen alignment of chromophores. Then, the films were exposed to 365 nm UV light for 30 min. And there was always a high voltage applied during the process of poling and UV light. The photo-crosslinking process was repeated three times to ensure complete crosslinking, with the results summarized in Fig. S8 (ESI†). For films **DN-SH2** and **DN-SH5**, there was no obvious difference of $T_{80\%}$ between the two test methods, however, the d_{33} value can be greatly influenced by the temperature of illumination. The d_{33} value of **DN-SH2** (89 pm V^{-1}) is much higher than that of **DN-SH5** (75 pm V^{-1}) after photo cross-linking. For films **DS-SH2** and **DS-SH3**, although the **DS-SH3** film exhibited a little better NLO stability after photo crosslinking, the d_{33} value of **DS-SH3** (95 pm V^{-1}) is lower than that of **DS-SH2** (108 pm V^{-1}) after the crosslinking process, which is almost consistent with the results of **DN-SH** films. These results indicated that irradiation conditions (such as, temperature) can greatly influence the d_{33} value. It is easy to understand why the d_{33} value can be influenced. As we all know, the molecules are easier to move especially at a temperature approaching glass transition temperature. So, there should be an equilibrium state between the random motion of molecules and the orderly arrangement of molecules at a high voltage at the best poling temperature. When the molecules were in a state which is not beneficial to produce higher NLO activity, the molecules were locked through a thiol–ene reaction under UV light, resulting in a lower d_{33} value. In contrast, molecular orientation was "frozen" at room temperature with the application of an electric field and the molecules could not move freely, resulting in a relatively higher d_{33} value. Thus, it is better that the photo-crosslinking process was conducted at room temperature for 30 min.

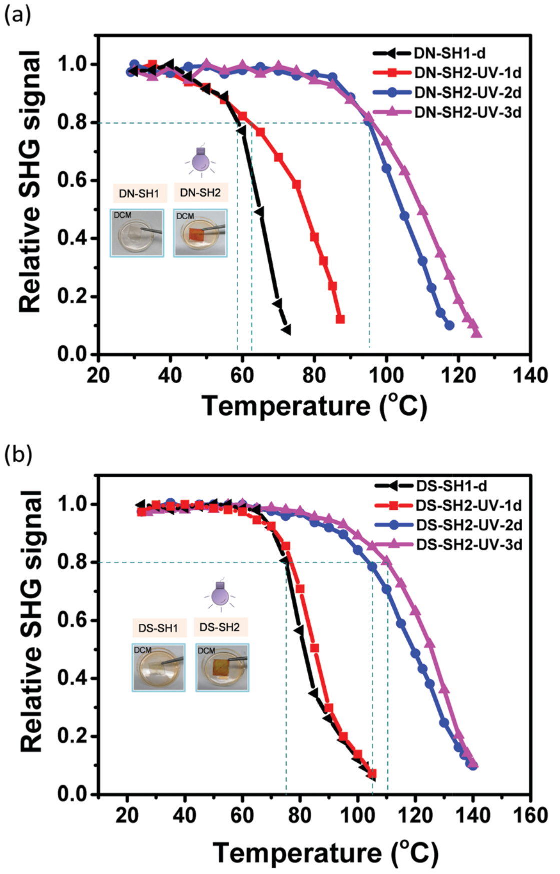

Fig. 4 Depoling curves of films **DN-SH1**, **DN-SH2** (illuminated at room temperature for 30 min), **DS-SH1** and **DS-SH2** (illuminated at room temperature for 30 min) and subsequent solubility tests (insert pictures).

The depoling curves of second-order nonlinear materials after poling were recorded to explore the optical stability of films by the real time decays of the SHG signals (Fig. 4). There was no electric field applied during the depoling process, and then the poled films were heated gradually from room temperature until no obvious signals were observed. As shown in Fig. 4(a), $T_{80\%}$ of **DN-SH2** after first depoling is 62.5 °C, slightly higher than that of **DN-SH1** (about 57.5 °C) without UV light irradiation, while in the second and third depoling, $T_{80\%}$ of **DN-SH2** gradually increased to 95 °C, much higher than that of **DN-SH1**. These results demonstrated that the thermostability of NLO property greatly enhanced after the photo-crosslinking process. Similarly, in Fig. 4(b), $T_{80\%}$ of photo-crosslinked **DS-SH2** increased from 77.5 °C to 110 °C after three times of depoling, much higher than that of uncrosslinked **DS-SH1** (75 °C). Thus, the photo-crosslinking process can indeed improve the thermostability of NLO property, and it is very convenient to control this process unlike thermo-crosslinking.

Also, the solubility tests of films were conducted to monitor the crosslinking process. As shown in Fig. 4 (inserted small pictures), there are four pictures of uncrosslinked and crosslinked films which have undergone the poling and depoling process, immerged in dichloromethane. First **DN-SH2** was exposed to UV light for 30 min, and then **DN-SH1** was tested without UV irradiation for comparison. The **DN-SH1** film is almost completely soluble in dichloromethane. By contrast, the **DN-SH2** film after being irradiated with UV light is only a little soluble in dichloromethane. In the same way, the poor solubility of film **DS-SH2** in dichloromethane also indicated thiol–ene reactions occurring under 365 nm UV light, without photo-initiators. A free radical-induced thiol–ene click reaction has been widely applied in protective coatings and films, because of its enormous advantages, such as high efficiency, no by-products, insensitivity to oxygen and so on.[12] This reaction involves the process of chain initiation and chain transfer which can form polymers with larger molecular weight. Besides, the thickness of the films we prepared is about 200 nm and high-intensity UV light makes the thiol group react with double bonds quickly, and the chromophore moieties are easier to move under a high electric field at the same time. Thus, insoluble polymers were obtained.

Besides, under the optimized conditions, the doping experiments were also carried out. Monomers **DN-SH** and **DS-SH** were mixed at molar ratios of 1 : 1, 1 : 2 and 2 : 1 respectively. The poling and depoling curves of doped systems are shown in Fig. S9–S11 (ESI†), with the results summarized in Fig. 5. All the doped films, which were irradiated for 30 min at room temperature after poling, demonstrated obviously enhanced NLO thermostability compared to that of uncrosslinked doped ones, in agreement with that of the single component.

According to the experimental data, the d_{33} values of photo-crosslinked films **DN-SH**, **DS-SH** and doped systems were calculated, respectively. As shown in Fig. 6, the d_{33} value of the crosslinked film of **DS-SH** (108 pm V^{-1}) is higher than that of **DN-SH** (89 pm V^{-1}), owing to the presence of sulfonyl-based chromophores which can decrease the dipole–dipole interactions between azo-based chromophores. Excitedly, all doped systems (1 : 1 doped, 2 : 1 doped, and 1 : 2 doped) showed better NLO properties with d_{33} values up to 123, 122, and 114 pm V^{-1}, respectively, after photo-crosslinking, in comparison with that of the single component. For doped systems, the density of the azo-based chromophores increased in comparison with single **DS-SH**, and meanwhile the sulfonyl-based chromophore can also act as an isolation chromophore to decrease the strong

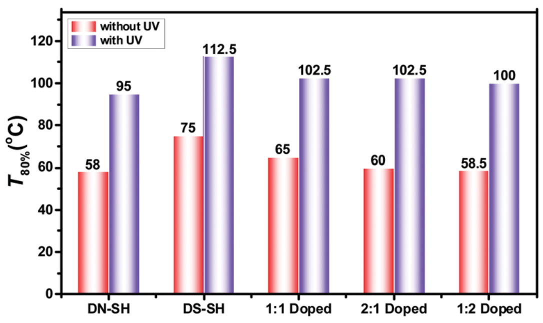

Fig. 5 $T_{80\%}$ of films **DN-SH**, **DS-SH** and 1 : 1 doped, (**DN-SH** : **DS-SH**, 1 : 1, M : M), 2 : 1 doped (**DN-SH** : **DS-SH**, 2 : 1, M : M), and 1 : 2 doped (**DN-SH** : **DS-SH**, 1 : 2, M : M) with and without photo-crosslinking processes.

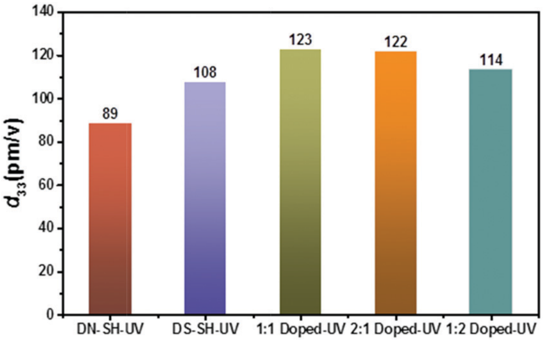

Fig. 6 d_{33} values of films **DN-SH2**, **DS-SH2** and 1 : 1 doped (**DN-SH** : **DS-SH**, 1 : 1, M : M), 2 : 1 doped (**DN-SH** : **DS-SH**, 2 : 1, M : M), and 1 : 2 doped (**DN-SH** : **DS-SH**, 1 : 2, M : M) after photo-crosslinking.

interactions between azo-based chromophores, leading to better NLO performance.

Conclusions

In summary, two AB_2-type monomers with alkyne and thiol as terminal groups were synthesized successfully. The films of **DS-SH** and **DN-SH** were respectively irradiated at different temperatures for 30 min by utilizing the thiol–ene click reaction. The photo-crosslinking process conducted at room temperature after poling showed better results, with the $T_{80\%}$ of **DS-SH** increasing from 75 before poling to 112.5 °C, while $T_{80\%}$ of the **DN-SH** film increased from 58 to 95 °C after poling. The doped films of **DN-SH** and **DS-SH** at a molar ratio of 1 : 1 showed larger NLO properties (123 pm V^{-1}) after the photo-crosslinking process than single **DN-SH** (89 pm V^{-1}) and **DS-SH** (108 pm V^{-1}). Thus, the utilization of photo-crosslinking is a promising method to achieve good NLO stability and relatively large NLO properties simultaneously by regulating the balance between electrostatic interactions and molecular structures.

Experimental section

Materials

Dichloromethane was dried with CaH_2 and distilled before use. Tetrahydrofuran (THF) was dried from K–Na alloy and distilled under an atmosphere of dry nitrogen. The synthetic routes of **1** and **2** are shown in the ESI.† All other reagents were used as received.

Instrumentation

^1H and ^{13}C NMR spectra were recorded on a Bruker AVANCE III HD 400 MHz spectrometer using tetramethylsilane (TMS; δ = 0 ppm) as the internal standard. High resolution mass spectra (HRMS) were measured on an LTQ-Orbitrap Elite high-resolution mass spectrometer equipped with an electrospray ionization (ESI†) source. UV-visible spectra were obtained using a Shimadzu UV-2550 spectrometer. The Fourier transform infrared (FTIR) spectra were recorded on a PerkinElmer-2 spectrometer in the region of 3000–400 cm^{-1} on KBr pellets. Thermogravimetric analysis (TGA) was performed on a NETZSCH STA449C thermal analyzer at a heating rate of 10 °C min^{-1} in nitrogen at a flow rate of 50 cm^3 min^{-1}. Differential scanning calorimetry (DSC) was investigated using DSC Q2000 V24.11 Build 124 under nitrogen at a scanning rate of 10 °C min^{-1}. Elemental analysis (EA) was performed using a CARLOERBA-1106 micro-elemental analyzer.

Synthesis

DN-OH. Compound **1** (200 mg, 0.40 mmol), **2** (363.58 mg, 0.926 mmol), $CuSO_4 \cdot 5H_2O$ (10% mol), $NaHCO_3$ (20% mol) and ascorbic acid (20% mol) were added into a Schlenk flask. THF (9 mL) and water (1.8 mL) were added to react for 3 h under nitrogen at room temperature. Then the reaction solution was extracted by water, and the solvent was removed by rotary evaporation. The crude product was purified by column chromatography on silica gel using dichloromethane and ethyl acetate (1/1.5) as eluents, to yield a red solid (400 mg, 78%). ^1H NMR (400 MHz, $CDCl_3$, 298 K), δ (TMS, ppm): 1.24 (t, J = 8.0 Hz, 6H, $-CH_3$), 1.62–1.39 (m, 6H, $-CH_2-$), 1.91 (m, 2H, $-CH_2-$), 2.21 (m, 4H, $-CH_2-$), 2.70 (s, 1H, –OH), 2.95 (t, J = 4.0 Hz, 4H, $-CH_2-$), 3.47 (q, 4H, $-CH_2-$), 3.73–3.65 (m, 6H, $-CH_2-$), 4.19–4.01 (m, 10H, $-CH_2-$), 4.38 (t, J = 4.0 Hz, 4H, $-CH_2-$), 5.20–5.14 (m, 4H, $-C{=}CH_2$), 5.81–5.88 (m, 2H, $-CH{=}C$), 6.48 (d, J = 8.0 Hz, 2H, ArH), 6.70 (d, J = 8.0 Hz, 4H, ArH), 7.23 (s, 2H, $-C{=}CH-$), 7.95–7.46 (m, 15H, ArH). ^{13}C NMR (100 MHz, CD_2Cl_2, 298 K), δ (ppm): 155.77, 155.06, 151.64, 149.55, 148.70, 148.00, 147.14, 147.09, 146.34, 145.34, 144.11, 132.99, 126.06, 125.82, 122.40, 117.13, 116.97, 116.43, 116.12, 116.00, 111.70, 111.46, 109.33, 109.15, 70.02, 68.69, 62.37, 52.62, 51.16, 47.31, 45.36, 32.94, 29.11, 28.52, 26.10, 25.64, 21.75, 12.21. HRMS (ESI, m/z): calcd for $C_{66}H_{77}N_{18}O_{10}$: 1281.6065 $[M + H]^+$; found: 1281.6060.

DN-S-S-DN. **DN-OH** (236 mg, 0.18 mmol), 3,3′-dithiodipropionic acid (19.36 mg, 0.09 mmol), EDC (52.96 mg, 0.27 mmol) and DMAP (30% mol) were added in distilled dichloromethane (2.3 mL). The resultant mixture was stirred at 30 °C for 7 h. The organic layer was extracted by a citric acid aqueous solution and water, and then the solvent was removed by rotary evaporation. The crude product was purified by column chromatography on silica gel using dichloromethane and ethyl acetate eluents (1/1), to yield a red solid (150 mg, 61%). ^1H NMR (400 MHz, $CDCl_3$, 298K), δ (TMS, ppm): 1.23 (t, J = 8.0 Hz, 12H, $-CH_3$), 1.65–1.46 (m, 12H, $-CH_2-$), 1.92 (m, 4H, $-CH_2-$), 2.23 (m, 8H, $-CH_2-$), 2.67 (t, J = 8.0 Hz, 4H, $-CH_2-$), 2.85 (t, J = 8.0 Hz, 4H, $-CH_2-$), 2.95 (t, J = 8.0 Hz, 8H, $-CH_2-$), 3.48 (q, 8H, $-CH_2-$), 3.71 (t, J = 8.0 Hz, 8H, $-CH_2-$), 4.00 (t, J = 4.0 Hz, 8H, $-CH_2-$), 4.19–4.06 (m, 16H, $-CH_2-$), 4.37 (t, J = 8.0 Hz, 8H, $-CH_2-$), 5.20–5.13 (m, 8H, $-C{=}CH_2$), 5.88–5.81 (m, 4H, $-CH{=}C$), 6.58 (d, J = 12.0 Hz, 4H, ArH), 6.69 (d, J = 8.0 Hz, 8H, ArH), 7.63–7.57 (m, 6H, ArH), 7.84–7.75 (m, 24H, ArH). ^{13}C NMR (100 MHz, $CDCl_3$, 298 K), δ (ppm): 171.77, 155.54, 154.90, 151.57, 149.18, 148.60, 147.90, 147.21, 147.18, 146.34, 145.34, 144.20, 132.72, 126.30, 126.11, 122.43, 117.37, 117.32, 116.64, 116.57, 116.23, 111.72, 111.45, 109.19, 108.96, 69.78, 68.54, 64.79, 52.67, 51.30, 47.25, 45.37, 34.05, 33.13, 28.88, 28.51, 28.40, 25.72, 25.70, 21.87, 12.50. EA: (%, found/calcd): C, 60.59/60.56; H, 5. 62/5.82; N, 18.17/18.42; S, 2.06/2.34.

DN-SH. Under an atmosphere of nitrogen, **DN-S-S-DN** (135 mg, 0.05 mmol), DTT (16.74 mg, 0.11 mmol), Et$_3$N (11.33 mg, 0.11 mmol) and distilled dichloromethane (2 mL) were added into a Schlenk flask. The reaction mixture was stirred at room temperature for 5 h. The organic layer was washed with HCl (0.1 mol L^{-1}) and water, and the solvent was removed by rotary evaporation. The crude product was purified by column chromatography on silica gel using dichloromethane and ethyl acetate as eluents (2/1), to yield a red solid (60 mg, 44%). ^{1}H NMR (400 MHz, CDCl$_3$, 298 K), δ (TMS, ppm): 1.24 (t, J = 4.0 Hz, 6H, –CH$_3$), 1.71–1.48 (m, 7H, –CH$_2$–, SH), 1.95–1.90 (m, 2H, –CH$_2$–), 2.24 (m, 4H, –CH$_2$–), 2.60 (t, J = 8.0 Hz, 2H, –CH$_2$–), 2.71 (q, 2H, –CH$_2$–), 2.96 (t, J = 8.0 Hz, 4H, –CH$_2$–), 3.48 (q, 4H, –CH$_2$–), 3.73 (t, J = 4.0 Hz, 4H, –CH$_2$–), 4.00 (t, J = 4.0 Hz, 4H,–CH$_2$–), 4.20–4.09 (m, 8H, –CH$_2$–), 4.38 (t, J = 8.0 Hz, 4H, –CH$_2$–), 5.18 (m, 4H, –C=CH$_2$), 5.88–5.81 (m, 2H, –CH=C), 6.59 (d, J = 8.0 Hz, 2H, ArH), 6.70 (d, J = 8.0 Hz, 4H, ArH), 7.63–7.58 (m, 3H, ArH), 7.85–7.76 (m, 12H, ArH). ^{13}C NMR (100 MHz, CDCl$_3$), δ (TMS, ppm): 171.74, 155.55, 154.90, 151.58, 149.18, 148.62, 147.90, 147.22, 147.19, 146.36, 145.36, 144.20, 132.72, 126.30, 126.12, 122.42, 117.37, 117.33, 116.64, 117.57, 116.23, 111.73, 111.46, 109.20, 108.95, 69.78, 68.55, 64.68, 52.67, 51.30, 47.26, 45.37, 38.47, 28.89, 28.53, 28.41, 25.76, 25.71, 21.87, 19.80, 12.50. HRMS (ESI, m/z): calcd for $C_{69}H_{81}N_{18}O_{11}S$: 1369.6047 $[M + H]^+$; found: 1369.6033. EA (%, found/calcd): C, 60.2/60.51; H, 5.601/5.89; N, 18.32/18.41; S, 2.163/2.34.

Preparation of films

The monomers **DN-SH** and **DS-SH**, and doped systems were dissolved in dichloromethane respectively with the concentration of 30 mg mL^{-1}, and the solutions were filtered by syringe filters. Then the solution was spin-coated onto indium-tin-oxide (ITO)-coated glass substrates to give thick films. These glass substrates were cleaned by ultrasonic treatment in different solvents of water, acetone, deionized water, DMF, and THF before use. Finally, thin films were heated in a vacuum oven at 45 °C to remove residual solvents.

NLO measurements and photo-crosslinking of monomers

The second-order optical nonlinearity of the materials was conducted by an *in situ* second harmonic generation (SHG) experiment by using a closed temperature-controlled oven with optical windows and three needle electrodes. The films were kept at 45° to the incident beam and poled inside the oven, and the SHG intensity was monitored simultaneously. The SHG measurements were carried out with an Nd:YAG laser operating at a 10 Hz repetition rate and an 8 ns pulse width at 1064 nm. The poling voltage is 7 kV. The temperature was different for different monomers.

The thin films were heated to the best poling temperature (T_e) under the electric field. After maintaining for 10 min at T_e, the photo-crosslinking process was conducted immediately or at room temperature. The poled films were exposed to the 365 nm UV light for 30 min with the voltage applied, and then the photo-crosslinked films were obtained.

The depoling curves of second-order nonlinear materials after poling were conducted as follows: poled films were heated gradually from room temperature until no obvious signals were observed. The heating rate was 4 °C min^{-1}. $T_{80\%}$ represents the temperature at which the SHG signals decreased to initial 80%.

Conflicts of interest

There are no conflicts to declare.

Acknowledgements

We are grateful to the National Natural Science Foundation of China (21734007) for financial support.

Notes and references

1 S. R. Marder, B. Kippelen, A. K. Y. Jen and N. Peyghambarian, *Nature*, 1997, **388**, 845; C. V. McLaughlin, L. M. Hayden, B. Polishak, S. Huang, J. Luo, T.-D. Kim and A. K. Y. Jen, *Appl. Phys. Lett.*, 2008, **92**, 151107; S. Huang, J. Luo, Z. Jin, X.-H. Z. Z. Shi and A. K. Y. Jen, *J. Mater. Chem. C*, 2012, **22**, 20353; M. J. Cho, D. H. Choi, P. A. Sullivan, A. J. P. Akelaitis and L. R. Dalton, *Prog. Polym. Sci.*, 2008, **33**, 1013; K. Clays and B. J. Coe, *Chem. Mater.*, 2003, **15**, 642; Y. Bai, N. Song, J. P. Gao, X. Sun, X. Wang, G. Yu and Z. Y. Wang, *J. Am. Chem. Soc.*, 2005, **127**, 2060; D. M. Burland, R. D. Miller and C. A. Walsh, *Chem. Rev.*, 1994, **94**, 31; Q. Li and Z. Li, *Acc. Chem. Res.*, 2020, **53**, DOI: 10.1021/acs.accounts.0c00060.

2 M. Lee, H. E. Katz, C. Erben and D. M. Gill, *Science*, 2002, **298**, 1401; L. R. Dalton, P. A. Sullivan and D. H. Bale, *Chem. Rev.*, 2010, **110**, 25; C. Ji, Z. Sun, S. Zhang, S. Zhao, T. Chen, Y. Tang and J. Luo, *Chem. Commun.*, 2015, **51**, 2298; Y. Cheng, J. Luo, S. Huang, X. Zhou, Z. Shi, T.-D. Kim, D. H. Bale, S. Takahashi, A. Yick, B. M. Polishak, S.-H. Jang, L. R. Dalton, P. J. Reid, W. H. Steier and A. K. Y. Jen, *Chem. Mater.*, 2008, **20**, 5047; J. Luo, Y.-J. Cheng, T.-D. Kim, S. Hau, S.-H. Jang, Z. Shi, X.-H. Zhou and A. K. Y. Jen, *Org. Lett.*, 2006, **8**, 1387.

3 F. Wang, A. W. Harper, M. S. Lee and L. R. Dalton, *Chem. Mater.*, 1999, **11**, 2285; T.-A. Chen, A. K.-Y. Jen and Y. Cai, *J. Am. Chem. Soc.*, 1995, **117**, 7295; W. Jin, P. V. Johnston, D. L. Elder, K. T. Manner, K. E. Garrett, W. Kaminsky, R. Xu, B. H. Robinson and L. R. Dalton, *J. Mater. Chem. C*, 2016, **4**, 3119; D. Yu, A. Gharavi and L. Yu, *J. Am. Chem. Soc.*, 1995, **117**, 11680; T. J. Marks and M. A. Ratner, *Angew. Chem., Int. Ed. Engl.*, 1995, **34**, 155.

4 J. Zhou, M. Wang, A. A. Fedorchuk, I. V. Kityk and J. Liu, *J. Mater. Sci: Mater. Electron.*, 2017, **28**, 4931; M. H. Davey, V. Y. Lee, L.-M. Wu, C. R. Moylan, W. Volksen, A. Knoesen, R. D. Miller and T. J. Marks, *Chem. Mater.*, 2000, **12**, 1679; A. Scarpaci, E. Blart, V. Montembault, L. Fontaine,

V. Rodriguez and F. Odobel, *Chem. Commun.*, 2009, 1799; J.-F. Wang, L. Geng, W. Lin, T. J. Marks and G. K. Wong, *Mater. Res. Soc. Symp. Proc.*, 1995, **392**, 85.

5 Z. Shi, S. Hau, J. Luo, T.-D. Kim, N. M. Tucker, J.-W. Ka, H. Sun, A. Pyajt, L. Dalton, A. Chen and A. K.-Y. Jen, *Adv. Funct. Mater.*, 2007, **17**, 2557; P. A. Sullivan, B. C. Olbricht, A. J. P. Akelaitis, A. A. Mistry, Y. Liao and L. R. Dalton, *J. Mater. Chem.*, 2007, **17**, 2899; M. Haller, J. Luo, H. Li, T.-D. Kim, Y. Liao, B. H. Robinson, L. R. Dalton and A. K. Y. Jen, *Macromolecules*, 2004, **37**, 688; Z. Shi, W. Liang, J. Luo, S. Huang, B. M. Polishak, X. Li, T. R. Younkin, B. A. Block and A. K. Y. Jen, *Chem. Mater.*, 2010, **22**, 5601.

6 J. Lu and J. Yin, *J. Polym. Sci.*, 2003, **41**, 303; D. Zhang, J. Sun, J. Shen and M. Yi, *J. Appl. Polym. Sci.*, 2000, **77**, 1506; A. Godt, J. M. J. Fréchet, J. E. Beecher and C. S. Willand, *Macromol. Chem. Phys.*, 1995, **196**, 133; B. K. Mandal, Y. M. Chen, J. Y. Lee, J. T. Kumar and S. Tripathy, *Appl. Phys. Lett.*, 1991, **58**, 2459; D. H. Choi, S. Song, W. S. Jahng and N. Kim, *Mol. Cryst. Liq. Cryst.*, 1996, **280**, 17; M. J. Cho, S. K. Lee, D. H. Choi and J. Jin, *Dyes Pigm.*, 2008, **77**, 335.

7 J. A. F. Boogers, P. Th., A. Klaase, J. J. de Vlieger, D. P. W. Alkema and A. H. A. Tinnemans, *Macromolecules*, 1994, **27**, 197.

8 T. Goodson, J. M. Takacs, C. H. Wang and L. Zhang, *J. Nonlinear Opt. Phys. Mater.*, 1996, **5**, 437.

9 S. Ding, C. Wang, X. Shi, J. Zou, Q. Cheng, J. Zhu, Z. Shi, Z. Cai, C. Chen and Z. Cui, *J. Mater. Chem. C*, 2019, **7**, 4667.

10 Z. Li, Z. Li, C. Di, Z. Zhu, Q. Li, Q. Zeng, K. Zhang, Y. Liu, C. Ye and J. Qin, *Macromolecules*, 2006, **39**, 6951.

11 W. Wu, Li. Huang, C. Song, G. Yu, C. Ye, Y. Liu, J. Qin, Q. Li and Z. Li, *Chem. Sci.*, 2012, **3**, 1256; Z. Li, W. Wu, C. Ye, J. Qin and Z. Li, *Polymer*, 2012, **53**, 153; W. Wu, Z. Wang, R. Xiao, Z. Xu and Z. Li, *Polym. Chem.*, 2015, **6**, 4369; W. Wu, Z. Xu, W. Xiang and Z. Li, *Polym. Chem.*, 2014, **5**, 6667; W. Wu, Z. Xu and Z. Li, *J. Mater. Chem. C*, 2014, **2**, 8122; P. Chen, H. Zhang, M. Han, Z. Cheng, Q. Peng, Q. Li and Z. Li, *Mater. Chem. Front.*, 2018, **2**, 1374; P. Chen, G. Liu, H. Zhang, M. Jin, M. Han, Z. Cheng, Q. Peng, Q. Li and Z. Li, *J. Mater. Chem. C*, 2018, **6**, 6784; H. Yang, Z. Cheng, C. Liu, W. Wu, K. Zhang, S. Xu, Y. Liu, S. Cao and Z. Li, *Sci. China: Chem.*, 2018, **61**, 584.

12 O. Z. Durham, D. V. Chapman, S. Krishnan and D. A. Shipp, *Macromolecules*, 2017, **50**, 775; Y. Li, M. Ren, P. Lv, Y. Liu, H. Shao, C. Wang, C. Tang, Y. Zhou and M. Shuai, *J. Mater. Chem. A*, 2019, **7**, 7242; S. V. Radl, C. Schipfer, S. Kaiser, A. Moser, B. Kaynak, W. Kern and S. Schlögl, *Polym. Chem.*, 2017, **8**, 9; L. Chen, Q. Wu, G. Wei, R. Liu and Z. Li, *J. Mater. Chem. C*, 2018, **6**, 43; C. E. Hoyle and C. N. Bowman, *Angew. Chem., Int. Ed.*, 2010, **49**, 1540; Y. Tian, Q. Wang, J. Cheng and J. Zhang, *Green Chem.*, 2020, **22**, 921.

13 Z. Cheng, R. Tang, R. Wang, Y. Xie, P. Chen, G. Liu and Z. Li, *Polym. Chem.*, 2018, **9**, 3522.

14 W. Wu, J. Qin and Z. Li, *Polymer*, 2013, **54**, 4351; W. Wu, C. Wang, R. Tang, Y. Fu, C. Ye, J. Qin and Z. Li, *J. Mater. Chem. C*, 2013, **1**, 717; R. Tang, S. Zhou, Z. Cheng, G. Yu, Q. Peng, H. Zeng, G. Guo, Q. Li and Z. Li, *Chem. Sci.*, 2017, **8**, 340; R. Tang, H. Chen, S. Zhou, B. Liu, D. Gao, H. Zeng and Z. Li, *Polym. Chem.*, 2015, **6**, 6680.

15 J. Z. Liu, J. W. Y. Lam and B. Z. Tang, *Chem. Rev.*, 2009, **109**, 5709; A. J. Qin, L. Tang, J. W. Y. Lam, C. K. W. Jim, Y. Yu, H. Zhao, J. Z. Sunand and B. Z. Tang, *Adv. Funct. Mater.*, 2009, **19**, 1891; A. Qin, J. W. Y. Lam and B. Tang, *Chem. Soc. Rev.*, 2010, 39–2522.

16 G. Liu, Q. Liao, H. Deng, W. Zhao, P. Chen, R. Tang, Q. Li and Z. Li, *J. Mater. Chem. C*, 2019, **7**, 7344; R. Tang, H. Chen, S. Zhou, W. Xiang, X. Tang, B. Liu, Y. Dong, H. Zeng and Z. Li, *Polym. Chem.*, 2015, **6**, 5580.

17 G. Li, Z. Zhao, J. Liu and G. Jiang, *J. Hazard. Mater.*, 2011, **192**, 277.